**DTU Library**

# All passive synchronized Q-switching of a quasi-three-level and a four-level Nd:YAG laser

**Cheng, Haynes Pak Hay; Tidemand-Lichtenberg, Peter; Jensen, Ole Bjarlin; Andersen, Peter E.; Petersen, Paul Michael; Pedersen, Christian**

[Link back to DTU Orbit](Link back to DTU Orbit)

# All passive synchronized Q-switching of a quasi-three-level and a four-level Nd:YAG laser

**Haynes Pak Hay Cheng,\* Peter Tidemand-Lichtenberg, Ole Bjarlin Jensen, Peter Eskil Andersen, Paul Michael Petersen, and Christian Pedersen**

*DTU Fotonik, Technical University of Denmark, Frederiksborgvej 399, DK-4000, Roskilde, Denmark*
*\*hach@fotonik.dtu.dk*

**Abstract:** Using an all passive approach, synchronized Q-switching of two Nd:YAG lasers, at 946 nm and 1064 nm, is reported. Two laser crystals are used to avoid gain competition, and stable operation is reported for the first time. The pulse trains are synchronized over a wide range of pump powers and a relative timing jitter of 36 ns is achieved. A minimum delay of 64 ns is observed between the two laser pulses, and by making the 946 nm pulse relatively long, a 79% temporal overlap is obtained when compared to the zero-delay scenario.

## References and links

1. R. W. Farley, and P. D. Dao, "Development of an intracavity-summed multiple-wavelength Nd:YAG laser for a rugged, solid-state sodium lidar system," Appl. Opt. **34**(21), 4269–4273 (1995).
2. E. Herault, M. Lelek, F. Balembois, and P. Georges, "Pulsed blue laser at 491 nm by nonlinear cavity dumping," Opt. Express **16**(24), 19419–19426 (2008).
3. P. Tidemand-Lichtenberg, J. Janousek, R. Melich, J. L. Mortensen, and P. Buchhave, "Synchronization of 1064 and 1342 nm pulses using passive saturable absorbers," Opt. Commun. **241**(4-6), 487–492 (2004).
4. J. Janousek, P. Tidemand-Lichtenberg, J. L. Mortensen, and P. Buchhave, "Investigation of passively synchronized dual-wavelength Q-switched lasers based on V:YAG saturable absorber," Opt. Commun. **265**(1), 277–282 (2006).
5. X. Zhang, A. Brenier, J. Wang, and H. Zhang, "Absorption cross-sections of Cr4+:YAG at 946 and 914 nm," Opt. Mater. **26**(3), 293–296 (2004).
6. L. Zhang, Z. Wei, B. Feng, D. Li, and Z. Zhang, "Simultaneous dual-wavelength Q-switched Nd:YAG laser operating at 1.06 µm and 946 nm," Opt. Commun. **264**(1), 51–54 (2006).
7. V. Kh. Bagdasarov, N. N. Denisov, A. A. Malyutin, and I. A. Chigaev, "Pulse synchronization in passively Q-switched lasers emitting at 1.053 and 1.064 µm," Quantum Electron. **39**(10), 887–890 (2009).
8. H. P. H. Cheng, O. B. Jensen, P. Tidemand-Lichtenberg, P. E. Andersen, P. M. Petersen, B. Sumpf, G. Erbert, and C. Pedersen, "Efficient quasi-three-level Nd:YAG laser at 946 nm pumped by a tunable external cavity tapered diode laser," Opt. Commun. **283**(23), 4717–4721 (2010).
9. M. Chi, O. B. Jensen, J. Holm, C. Pedersen, P. E. Andersen, G. Erbert, B. Sumpf, and P. M. Petersen, "Tunable high-power narrow-linewidth semiconductor laser based on an external-cavity tapered amplifier," Opt. Express **13**(26), 10589–10596 (2005).
10. W. P. Risk, "Modeling of longitudinally pumped solid-state lasers exhibiting reabsorption losses," J. Opt. Soc. Am. B **5**(7), 1412–1423 (1988).
11. I. D. Lindsay, and M. Ebrahimzadeh, "Efficient continuous-wave and Q-switched operation of a 946-nm Nd:YAG laser pumped by an injection-locked broad-area diode laser," Appl. Opt. **37**(18), 3961–3970 (1998).
12. Q. Li, S. Wang, S. Du, Y. Shi, J. Xing, D. Zhang, B. Feng, Z. Zhang, and S. Zhang, "Self-Q-switched and mode-locked 946 nm Cr,Nd:YAG laser," Opt. Commun. **281**(8), 2184–2188 (2008).

## 1. Introduction

Synchronized Q-switching has been an active field of research in recent years, including both actively and passively Q-switched systems [1–4]. Synchronization between a quasi-three-level and a four-level laser is particularly interesting for sum frequency generation into the blue spectral region [2] and pump-probe experiments [5]. This is, however, complicated by reabsorption losses, and in the case of Nd:YAG, a seven times lower emission cross-section for the quasi-three-level transition.

There has been one demonstration of a pulsed simultaneous dual-wavelength laser (SDWL) at 1064 nm and 946 nm [6]; but due to gain competition in using a single laser crystal, considerable fluctuations in output powers were reported.

In another approach, a quasi-three-level 912 nm and a four-level 1063 nm Nd:GdVO$_4$ laser were synchronized using two laser crystals and two active Q-switches. The 912 nm pulses were made relatively long (250 ns) to absorb the relative jitter between the two pulse trains [2]. The authors reported that a timing jitter of 40 ns resulted in 10% peak-to-peak fluctuation in the resulting SFG power.

Recently, two flash-lamp pumped four-level Q-switched lasers were passively synchronized by directing the output of one laser (master) to the Q-switch of the other (slave), also achieving good temporal overlap by making one pulse relatively long when compared to the other [7].

In another all passive system, Tidemand-Lichtenberg et al. and Janousek et al. achieved good control between the various synchronization states using two laser crystals and individually adjusting the pump powers to the respective crystals [3,4]. This was demonstrated for the synchronization of two four-level lasers using Nd:YVO$_4$ – at 1064 nm, and 1342 nm.

In this paper, we report for the first time stable, synchronized Q-switching between a quasi-three-level transition and a four-level transition in an all passive approach. In contrast to a previous system [6], two laser crystals were used to avoid gain competition, resulting in stable synchronization. The two lasers were synchronized over a wide-range of pump powers despite the difference in their respective repetition rates. While timing jitter in the free-running lasers were on the order of 10 μs, the relative jitter between the two pulse trains was only 36 ns, comparable to the actively synchronized system reported in [2]. A minimum delay of 64 ns was observed between the two laser pulses. Making the 946 nm pulse relatively long, a 79% temporal overlap was achieved when compared to the zero-delay scenario.

## 2. Experimental setup

Figure 1 illustrates the experimental setup. The HR facet of Nd:YAG1, mirrors M1, BS and M2 form the 946 nm cavity, while the HR facet of Nd:YAG2, mirrors M3 and M2 form the 1064 nm cavity. Synchronization of the two lasers is achieved with one saturable absorber (SA), placed in the common section between BS and M2, close to the beam waist located at M2. The SA is a 0.97 mm Brewster-cut Cr:YAG specified for 85% unsaturated transmission at 1064 nm at normal incidence. Taking into account the SA is oriented at Brewster's angle and using the absorption cross-sections published in [5], the unsaturated transmission at 1064 nm and 946 nm are 82% and 83% respectively. Similarly, the saturated excited state absorption are 6% and 8% at 1064 nm and 946 nm respectively. M1, a plane folding mirror coated for high transmission at 808 nm and high reflection at 946 nm, is inserted to minimize feedback to the tapered diode pump source. BS is the coupling mirror coated for high transmission at 1064 nm and high reflection at 946 nm. M2 is the output coupler, coated for 3% transmission at both 1064 nm and 946 nm. M3, with a radius of curvature of 100 mm, is coated for high reflection at 1064 nm, and the intracavity lens, LS, with a focal length of 75 mm, is coated for high transmission at 946 nm. The cavity lengths are 19 cm and 37 cm for the 1064 nm and 946 nm lasers, respectively.

A narrow spectrum, external cavity tapered diode laser, at 808.8 nm, is used to pump the 946 nm laser, and is illustrated in the dotted red box in Fig. 1. The pump source has an M$^2$ of 1.4 and 5.7 for the fast and slow axis respectively (using the second-moments definition). After the optical isolators and focusing optics, 1.6 W of pump power is incident on the laser crystal (Nd:YAG1). Given the relatively large pump volume required for low-repetition rate, high pulse energy Q-switching, using a standard broad-area diode pump source should give similar performance. More detailed description on the external cavity tapered diode pump source can be found in [8,9]. The dotted green box illustrates the 1064 nm laser pump source, a fiber-pigtailed broad area diode laser (LUMICS LU0808T045) with NA = 0.15 and a fiber core diameter of 105 μm. It provides up to 4.1 W of incident power after the coupling optics.

The single-pass pump absorption through the 3 mm long 946 nm laser crystal (Nd:YAG1) and the 5 mm long 1064 nm laser crystal (Nd:YAG2) were 90% and 47% respectively. The relatively low absorption in the 1064 nm laser crystal is due a mismatch between the diode pump source spectrum and the absorption peak of Nd:YAG. The center wavelength of the broad area diode pump source is 801 nm, with a FWHM spectral bandwidth of 2.5 nm.
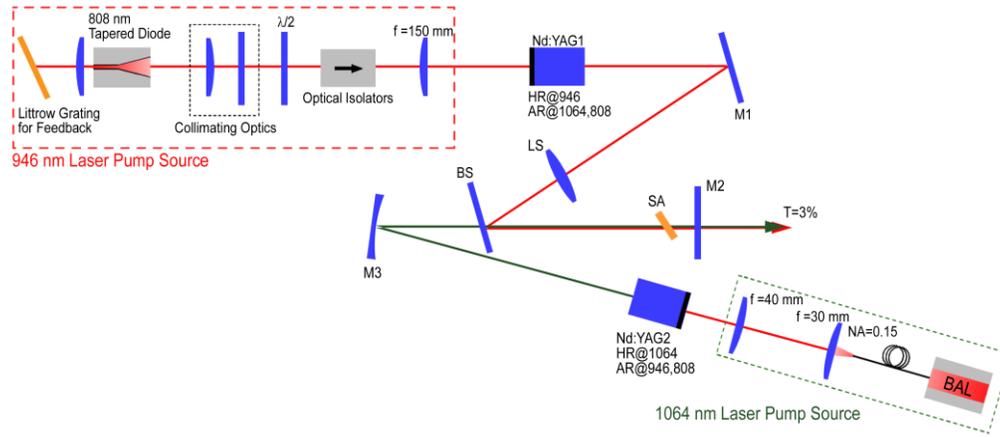


Fig. 1. (Color online) Experimental setup for synchronized Q-switching. Nd:YAG1 and Nd:YAG2 are the laser crystals for 946 nm and 1064 nm, respectively. SA is the saturable absorber that is shared between the two lasers.

The SA was placed close to the cavity beam waists at mirror M2, and the corresponding waist radii were measured with a Thorlabs BP109-IR beam profiler. They were 24 μm in both the horizontal and vertical directions for the 946 nm laser, and 72 μm (h) x 97 μm (v) for the 1064 nm laser.

The pump and cavity mode sizes inside the laser crystals were optimized experimentally. The cavity waist radii inside the laser crystals were estimated to be 77 μm (in both directions) and 88 μm (h) x 108 μm (v) for the 946 nm and 1064 nm lasers respectively. The tapered diode pump beam waist radius was measured to be 59 μm (h) x 80 μm (v), while the broad area diode pump beam waist radius was estimated to be 70 μm in both directions from the specified fiber core size and NA.

To overcome reabsorption loss at the 946 nm transition, a high pump photon density and a good overlap between the pump and cavity beams are required inside the laser crystal [10,11]. In addition, a small cavity mode inside the SA is desired for efficient bleaching and coupling of the two beams. These requirements imply the 946 nm laser only operates in a narrow range of cavity lengths near the stability limit. Thus, an intracavity lens, LS, was used instead of a curved folding mirror to avoid astigmatism, which would have produced asymmetric stability regions. The insertion loss of LS was measured to be 1.9%.

The pulsed signals were separated using dichroic beamsplitters and detected using two Thorlabs PDA-255 photodiodes, each with a 7 ns rise time. The respective signals were then captured using a LeCroy Wavesurfer 104MXs-A oscilloscope with 1 GHz bandwidth. It is reported previously that the 946 nm laser may simultaneously Q-switch and mode-lock when $Cr^{4+}$ ions are used in the SA [12]. This mode-locking behavior is not investigated in the current paper, and only the synchronized Q-switching process is considered.

## 3. Results and discussion

### 3.1 General system performance

Repetition rates of the synchronized system and of the respective free-running lasers at 946 nm and 1064 nm are plotted in Fig. 2, where the free-running repetition rates were measured with only one laser operating. The incident pump power of the 946 nm laser was held fixed at

1.6 W, while incident pump power of the 1064 nm laser was slowly increased from 0.69 W to 3.0 W. The threshold of the 1064 nm laser was reduced from 1.0 W of incident pump power in the free-running laser to 0.69 W in the synchronized system.

Operation of the synchronized system can be divided into three regimes: 1) when the free-running repetition rate of the 1064 nm laser is below that of the 946 nm laser, the SA is bleached by the 946 nm photons before sufficient gain in the 1064 nm laser is built up; thus, in this case, the 946 nm pump power determines the repetition rate of the synchronized laser. 2) When the free-running repetition rate of the 1064 nm laser is higher than that of the 946 nm laser, the 1064 nm laser bleaches the SA and its pump power determines the repetition rate of the synchronized laser. 3) When the free-running repetition rates of both lasers are matched, an unstable regime exists, where small changes in the two lasers' pulse build-up times become important. This regime will be discussed in the next section.
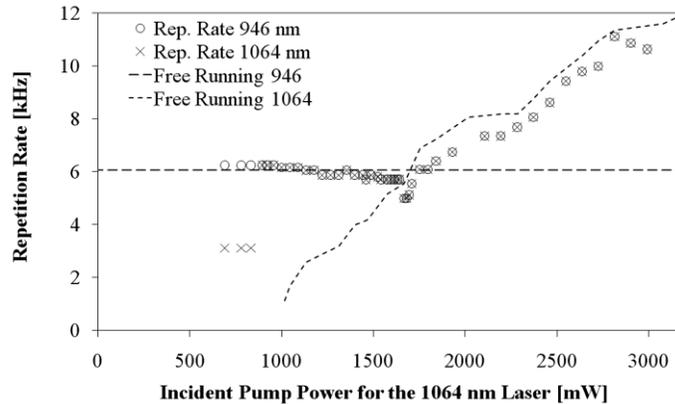


Fig. 2. Repetition rates of the synchronized system and of the respective free running lasers at 946 nm and 1064 nm.

Note that the first three data points in Fig. 2 indicate 2:1 synchronization, where the 1064 nm gain is so low that a 1064 nm pulse is only generated with every other 946 nm pulse. This is consistent with reports in [3,4]. It can be seen here, however, that the two lasers are locked together over a wide range of pump powers, with the 946 nm laser following the 1064 nm laser up to almost twice its natural free-running repetition rate.

When the 1064 nm laser pump power is increased beyond the switching point at ~1.6 W, both the average power and pulse energy of the 946 nm laser increased significantly, while the width of the Q-switch envelope decreased, as shown in Fig. 3. The relatively significant increase in performance of the 946 nm laser is due to the three-level nature of the laser line, where for each photon sacrificed for bleaching the SA, the population inversion is reduced by two. When this burden is taken by the 1064 nm laser, the excess gain in the 946 nm laser crystal could then be converted into useful output.

The second dip in the 1064 nm average power (at ~2.6 W) was due to thermal lensing, which caused the 1064 nm laser cavity to become unstable in the horizontal direction. This was verified using a beam profiler, where wings in the horizontal directions were observed in the 1064 nm laser mode at 2.6 W incident pump power. Higher order modes were observed when the pump power was further increased.

In the uploaded video (Media 1), the blue and yellow oscilloscope traces show the 1064 nm and 946 nm pulses, respectively. The 946 nm laser pump power was held at 1.6 W, while the 1064 nm laser pump power was increased in 0.1 A increments. Stable locking of the two lasers is clearly shown, and the abrupt change in output power is observed at 0:16 into the video.
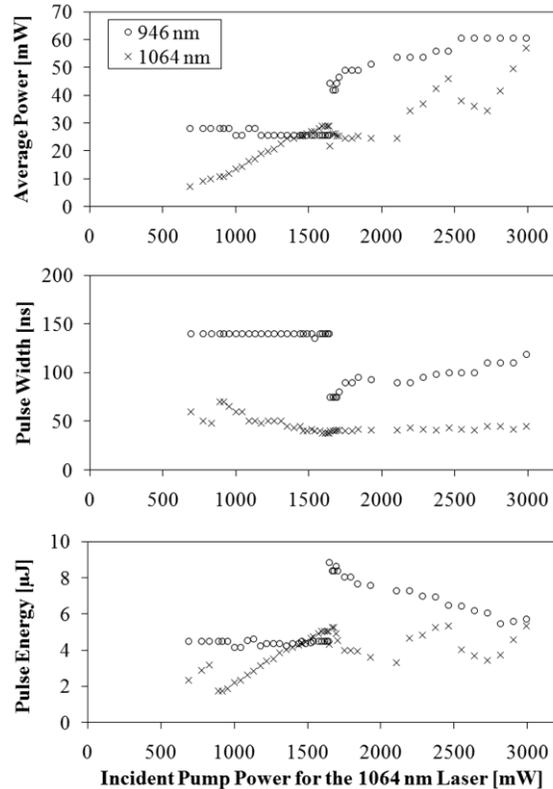
Fig. 3. Average power, Q-switch envelope width (FWHM), and pulse energy of the synchronized lasers.

## 3.2 Pulse delay and temporal overlap

Due to the unstable regime at around the switching point, a minimum delay between the two laser pulses was observed during stable operation. This delay is plotted in Fig. 4 (a) as a function of the 1064 nm laser pump power. A negative delay indicates the 1064 nm laser is lagging, while a positive delay indicates the 1064 nm laser is leading.

The general dependence of the delay on the 1064 nm laser pump power can be explained as follows: excess gain in the 1064 nm laser crystal, when the SA is bleached by the 946 nm laser, increases with the 1064 nm pump power; therefore the 1064 nm pulse build-up time decreases as a function of pump power, which in turn decreases the delay (regime 1). When the 1064 nm laser bleaches the SA at a higher repetition rate than the 946 nm laser, the two lasers switch roles and the 1064 nm laser becomes the leading pulse. As the pump power is further increased, the two pulses start to move apart in time again (regime 2). This also explains the drop in pulse energy and increase in the Q-switch envelope pulse width for the 946 nm laser as the 1064 nm pump power is increased beyond the switching point (see Fig. 3). Regime 3 is characterized by an abrupt change in delay in the experimental data. In order to better understand the physical mechanism responsible for the delay and in particular, the abrupt change in regime 3, a simple model based on coupled-rate equations [4] has been adapted for the three-level laser. The model shows qualitatively the pulse build-up and cavity losses in the three regimes as functions of time, shown in Fig. 4 (b) – (d). The absorbed pump power of the 1064 nm laser is increased by 100 mW in each subsequent plot, while the pump power of the 946 nm laser stays fixed.
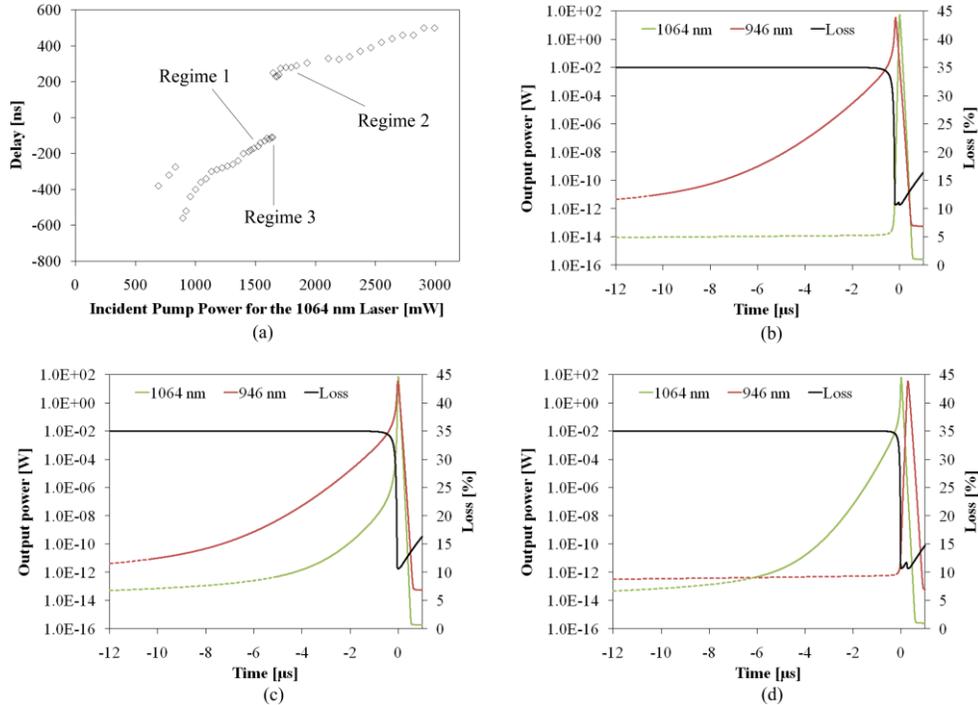
Fig. 4. (Color online) (a) Relative delay between the two laser pulses as a function of 1064 nm laser pump power, with the 946 nm laser pump power held at 1.6 W. Qualitative plots of the pulse build-up and cavity losses are shown for (b) regime 1, (c) regime 3, and (d) regime 2 as functions of time. Dashed lines in (b)-(d) indicate when the lasers are below threshold.

It can be seen in regime 1 (Fig. 4 (b)) that the 1064 nm laser does not reach threshold until the SA is bleached by the 946 nm laser, thus the point at which the 1064 nm laser reaches threshold is well defined. In regime 2 (Fig. 4(d)), the situation is reversed, and the 1064 nm pulse leads the 946 nm pulse. In regime 3 (Fig. 4 (c)), however, the free-running repetition rates of the two lasers are closely matched, and both lasers reach threshold before the SA is bleached. In this case, the photon flux for both lasers build up rapidly due to stimulated emission, and gain fluctuations that delay or advance the threshold on the order of microseconds will have a critical impact on the build-up time of the two pulses; thus, the theoretical minimum delay for stable operation depends on the jitter of the individual free-running lasers. Experimentally, the unstable regime 3 was observed to be very narrow, within tens of mW of incident pump power.

From experimental data, the minimum delay with stable operation was 84 ns when the 946 nm laser was bleaching the SA (regime 1) and 242 ns when the 1064 nm laser was bleaching the SA (regime 2). Measuring the delay over 1000 pulses and applying a Gaussian fit to the corresponding histogram, the 4-sigma timing jitter was found to be 36 ns and 55 ns for the corresponding operating points in regimes 1 and 2.

Reducing the 1064 nm mode size inside the SA, such that the horizontal beam waist radius matches that of the 946 nm laser (to 24 μm (h) x 80 μm (v)), reduced the minimum delay between the two pulses to 64 ns when the 946 nm laser was bleaching the SA. Figure 5 shows the corresponding oscilloscope trace. The jitter in this case was 48 ns using the 4-sigma definition. The focusing lens of the 1064 nm pump beam was changed from 40 mm to 20 mm in this experiment to suppress lasing of higher order modes. Further reduction of the 1064 nm SA mode size was not possible due to physical limits with the current setup.
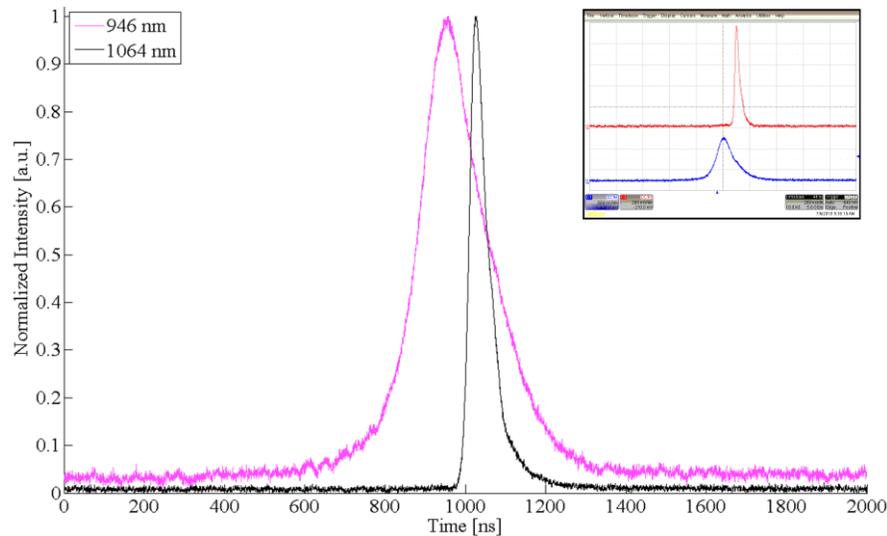
Fig. 5. (Color online) Oscilloscope traces of the two pulsed signals, showing good temporal overlap – black trace shows a 1064 nm pulse, purple trace shows a 946 nm pulse. The overlap corresponding to the product of the two pulses was 79% with respect to the best case scenario where no delay would be present. Inset shows a single frame in the uploaded video (Media 1) – upper trace shows a 1064 nm pulse, lower trace shows a 946 nm pulse.

By making one of the pulses relatively long compared to the other, good temporal overlap between the two could be achieved. It is reported in [2] that 40 ns of timing jitter in combination with a 250 ns long pulse resulted in less than 10% peak-to-peak fluctuation in the corresponding sum-frequency generation. In Fig. 5, the FWHM pulse widths of the 946 nm and 1064 nm lasers were 200 ns and 45 ns respectively. Multiplying the two traces, and integrating the resulting product over time, the temporal overlap between the two pulse trains was calculated to be 79%, with a 7% standard deviation. This was normalized against the best case scenario, where no delay between the two pulses would be present.

## 4. Conclusion

Stable synchronized Q-switching of a quasi-three-level and a four-level laser is demonstrated for the first time in an all passive approach. Stable locking of the two pulse trains was demonstrated over a wide range of pump powers. Relative timing jitter down to 36 ns was achieved, comparable to the 40 ns jitter reported in an actively synchronized system [2]. It was found that timing jitter in the individual free-running lasers would prevent perfect temporal overlap of the two pulse trains, but a minimum delay of 64 ns was achieved in stable operation. The relative timing jitter was absorbed into a 200 ns FWHM 946 nm pulse, and the resulting temporal overlap was 79% when compared to the best case scenario where no delay would be present. Based on the results presented, pump-probe experiments and sum-frequency generation based on passively synchronized Q-switching of quasi-three-level and four-level lasers seem feasible.

### Acknowledgement